

# Inverse design of next-generation superconductors using data-driven deep generative models

Daniel Wines,<sup>\*,†</sup> Tian Xie,<sup>‡</sup> and Kamal Choudhary<sup>†,¶</sup>

<sup>†</sup>*Material Measurement Laboratory, National Institute of Standards and Technology,  
Gaithersburg, Maryland 20899, USA*

<sup>‡</sup>*Microsoft Research AI4Science, Cambridge, United Kingdom CB1 2FB*

<sup>¶</sup>*DeepMaterials LLC, Silver Spring, MD 20906, USA*

E-mail: daniel.wines@nist.gov

## Abstract

Over the past few decades, finding new superconductors with a high critical temperature ( $T_c$ ) has been a challenging task due to computational and experimental costs. In this work, we present a diffusion model inspired by the computer vision community to generate new superconductors with unique structures and chemical compositions. Specifically, we used a crystal diffusion variational autoencoder (CDVAE) along with atomistic line graph neural network (ALIGNN) pretrained models and the Joint Automated Repository for Various Integrated Simulations (JARVIS) superconducting database of density functional theory (DFT) calculations to generate new superconductors with a high success rate. We started with a DFT dataset of  $\approx 1000$  superconducting materials to train the diffusion model. We used the model to generate 3000 new structures, which along with pre-trained ALIGNN screening results in 62 candidates. For the top candidate structures, we carried out further DFT calculations

to validate our findings. Such approaches go beyond the typical funnel-like materials design approaches and allow for the inverse design of next-generation materials.

**Keywords:** generative modeling; superconductivity; inverse design; density functional theory; high-throughput; materials discovery; machine learning

After superconductivity was discovered in 1911 by Onnes,<sup>1</sup> the efforts to identify novel superconducting materials with high transition temperatures ( $T_C$ ) has been an intense area of research in materials science and condensed matter physics.<sup>2,3</sup> There have been systematic computational efforts to identify Bardeen–Cooper–Schrieffer (BCS) conventional superconductors<sup>4,5</sup> with high- $T_C$  prior to costly experimental investigation,<sup>6,7</sup> where density functional theory-perturbation theory (DFT-PT) calculations have been performed to obtain the electron-phonon coupling (EPC) parameters. However, these typical funnel-like funnel screening-based approaches are not sufficient for inverse materials design, where instead of engineering from structure to property, the goal is to engineer from a target property to crystal structure.

The inverse design of novel materials becomes a difficult problem to solve due to the fact that there are an infinite number of possible materials with varying properties that are dependent on chemical composition and crystal structure. In order for inverse design to be successful, an algorithm that can successfully create new candidate structures based on a high quality and diverse dataset of materials data is required. There currently exists abundant sources of high quality calculated material properties in databases such as Materials Project,<sup>8</sup> Open Quantum Materials Database (OQMD),<sup>9,10</sup> C2DB<sup>11,12</sup> and our own JARVIS<sup>13</sup> database, which all contain millions of high-throughput<sup>13,14</sup> DFT calculations. The main obstacle in inverse design has been the method or algorithm used to generate new candidate materials. To circumvent this obstacle, generative machine learning algorithms can be used to successfully design new candidate structures. With the popularity of generative tools such as DALL-E,<sup>15</sup> which uses deep learning models to generate digital images from natural language descriptions (prompts), the interest in using deep generative mod-

els for scientific applications has immensely increased.<sup>16-19</sup> One of the main challenges with generative models for periodic materials stems from the creation of representations that are translationally and rotationally invariant.<sup>20-27</sup>

In a recent work, Xie et al. developed a crystal diffusion variational autoencoder (CDVAE) model<sup>17</sup> (<https://github.com/txie-93/cdvae>) for periodic structure generation. The CDVAE consists of a variational autoencoder<sup>28</sup> and a diffusion model<sup>29-31</sup> that works directly with the atomic coordinates of the structures and uses an equivariant graph neural network<sup>32</sup> to ensure invariance without the need for representations such as graphs or descriptors. The CDVAE consists of three simultaneously trained networks: 1) the encoder, which encodes onto the latent space, 2) the property predictor, which samples the latent space and predicts a structure and composition, and 3) the decoder, which is a diffusion model that denoises the randomly initialized atom types into a material that is similar to the training set distribution. More details of the CDVAE method can be found in Xie et al.<sup>17</sup> A recent work by Lyngby and Thygesen<sup>18</sup> successfully applied the CDVAE model to discover new, stable 2D materials and vastly expand the space of 2D materials (on the order of thousands). Another recent work by Moustafa et al.<sup>19</sup> used the CDVAE model to discover more than 500 new stable one-dimensional materials. In this work, we trained a CDVAE model with DFT computed data of 1058 superconducting materials from the JARVIS database and generated thousands of new candidate superconductors. We screened these candidate structures further by predicting the properties using pretrained deep learning models for fast predictions. After narrowing down the pool of potential candidate superconductors, we performed DFT calculations to verify our predictions and assessed the dynamical and thermodynamic stability of the newly predicted materials.

For deep learning predictions of EPC properties of superconductors, we used the recently developed atomistic line graph neural network (ALIGNN)<sup>33</sup> (<https://github.com/usnistgov/alignn>). The pretrained model for superconducting properties was specifically developed in ref.<sup>6</sup> ALIGNN, a crystal structure is represented as a graph using atomic ele-

ments as nodes and atomic bonds as edges. Each node in the atomistic graph is assigned 9 input node features based on its atomic species: electronegativity, group number, covalent radius, valence electrons, first ionization energy, electron affinity, block and atomic volume. The inter-atomic bond distances are used as edge features with radial basis function up to 8 Å cut-off. We use a periodic 12-nearest-neighbor ( $N$ ) graph construction. This atomistic graph is then used for constructing the corresponding line graph using interatomic bond-distances as nodes and bond-angles as edge features. ALIGNN uses edge-gated graph convolution for updating nodes as well as edge features using a propagation function ( $f$ ) for layer ( $l$ ), atom features ( $h$ ), and node ( $i$ ):

$$h_i^{(l+1)} = f(h_i^l \{h_j^l\}_i) \quad (1)$$

ALIGNN uses bond-distances as well as bond-angles to distinguish atomic structures. One ALIGNN layer composes an edge-gated graph convolution on the bond graph with an edge-gated graph convolution on the line graph. The line graph convolution produces bond messages that are propagated to the atomistic graph, which further updates the bond features in combination with atom features. The ALIGNN model is implemented in PyTorch<sup>34</sup> and deep graph library (DGL).<sup>35</sup> The hyperparameters for ALIGNN are kept same as the original paper.<sup>33</sup> For predicting the EPC parameters, we use a batch size of 16, 90:5:5 split and training for 300 epochs. The test set was never used during the training procedure.

We utilize the publicly available JARVIS<sup>13</sup> infrastructure for our DFT and deep learning goals mentioned above. JARVIS (Joint Automated Repository for Various Integrated Simulations, <https://jarvis.nist.gov/>) is a collection of databases and tools to automate materials design using classical force-field, density functional theory, machine learning calculations and experiments. JARVIS-DFT is a density functional theory based database of over 75000 materials with several material properties such as formation energy, band gap with different level of theories,<sup>36</sup> solar-cell efficiency,<sup>37</sup> topological spin-orbit coupling spillage,<sup>38-40</sup> elastic tensors,<sup>41</sup> dielectric tensors, piezoelectric tensors, infrared and Raman spectrum,<sup>42</sup>

electric field gradients,<sup>43</sup> exfoliation energies,<sup>44</sup> two-dimensional (2D) magnets,<sup>45</sup> and bulk<sup>6</sup> and 2D superconductors,<sup>7</sup> all with stringent DFT-convergence setup.<sup>46</sup> Our ALIGNN and CDVAE models were trained on the 1058 DFT calculations of superconducting properties presented in ref.<sup>6</sup>

To verify top candidate superconductors, we followed the workflow used to generate the training data (in ref.<sup>6</sup>), where we performed EPC calculations using non-spin polarized DFT-PT<sup>47,48</sup> (using the interpolated/Gaussian broadening method<sup>49</sup>) with the Quantum Espresso (QE) software package,<sup>50</sup> PBEsol functional,<sup>51</sup> and the GBRV<sup>52</sup> pseudopotentials. The EPC parameter is derived from spectral function  $\alpha^2 F(\omega)$  which is calculated as follows:

$$\alpha^2 F(\omega) = \frac{1}{2\pi N(\epsilon_F)} \sum_{qj} \frac{\gamma_{qj}}{\omega_{qj}} \delta(\omega - \omega_{qj}) w(q) \quad (2)$$

where  $\omega_{qj}$  is the mode frequency,  $N(\epsilon_F)$  is the DOS at the Fermi level  $\epsilon_F$ ,  $\delta$  is the Dirac-delta function,  $w(q)$  is the weight of the  $q$  point,  $\gamma_{qj}$  is the linewidth of a phonon mode  $j$  at wave vector  $q$  and is given by:

$$\gamma_{qj} = 2\pi\omega_{qj} \sum_{nm} \int \frac{d^3k}{\Omega_{BZ}} |g_{kn,k+qm}^j|^2 \delta(\epsilon_{kn} - \epsilon_F) \delta(\epsilon_{k+qm} - \epsilon_F) \quad (3)$$

Here, the integral is over the first Brillouin zone,  $\epsilon_{kn}$  and  $\epsilon_{k+qm}$  are the DFT eigenvalues with wavevector  $k$  and  $k + q$  within the  $n$ th and  $m$ th bands respectively,  $g_{kn,k+qm}^j$  is the electron-phonon matrix element.  $\gamma_{qj}$  is related to the mode EPC parameter  $\lambda_{qj}$  by:

$$\lambda_{qj} = \frac{\gamma_{qj}}{\pi h N(\epsilon_F) \omega_{qj}^2} \quad (4)$$

Now, the EPC parameter is given by:

$$\lambda = 2 \int \frac{\alpha^2 F(\omega)}{\omega} d\omega = \sum_{qj} \lambda_{qj} w(q) \quad (5)$$

with  $w(q)$  as the weight of a  $q$  point. The superconducting transition temperature,  $T_C$  can

then be approximated using McMillan-Allen-Dynes<sup>53</sup> equation as follows:

$$T_C = \frac{\omega_{log}}{1.2} \exp \left[ - \frac{1.04(1 + \lambda)}{\lambda - \mu^*(1 + 0.62\lambda)} \right] \quad (6)$$

where

$$\omega_{log} = \exp \left[ \frac{\int d\omega \frac{\alpha^2 F(\omega)}{\omega} \ln \omega}{\int d\omega \frac{\alpha^2 F(\omega)}{\omega}} \right] \quad (7)$$

In Eq. 6, the parameter  $\mu^*$  is the effective Coulomb potential parameter, which we take as 0.1. It is important to note that the robustness of this workflow was heavily benchmarked against experimental data and higher levels of theory in ref.<sup>6</sup> and,<sup>7</sup> which indicates that the training data for these deep learning models is of high quality, given the level of theory used to produce the data.

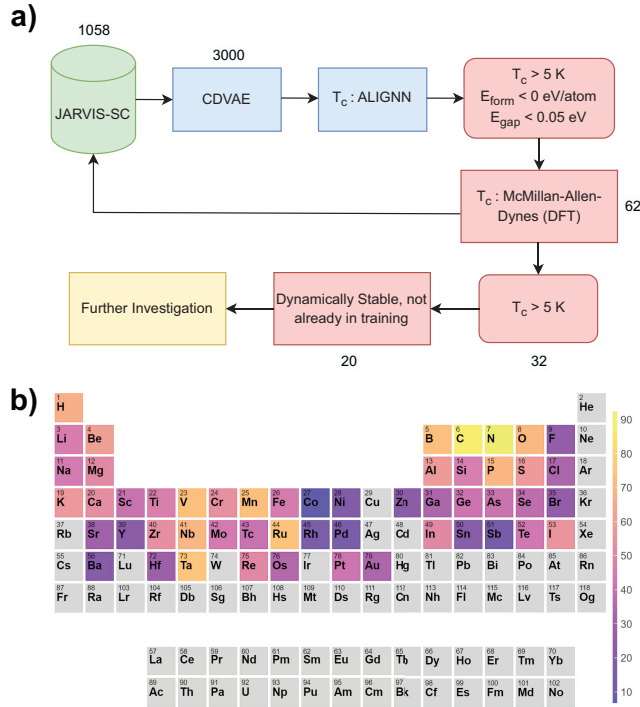


Figure 1: a) The full inverse design workflow for new superconductors using DFT, ALIGNN and the CDVAE generative model and b) the probability that compounds containing a given element in the CDVAE generated structures have an ALIGNN predicted  $T_C > 3$  K.

The full inverse design workflow proposed in this work is depicted in Fig. 1a). The first step of this workflow involved training the CDVAE model on the 1058 DFT calculations

in the JARVIS-SC (superconducting) database (from ref.<sup>6</sup>). With regards to the CDVAE model for inverse design, the target property to optimize was  $T_c$  for new candidate superconductors. After training on the JARVIS-SC data, we generated 3000 candidate materials using the CDVAE model. With such a large amount of crystal structures to investigate, it is impracticable to perform DFT calculations of the EPC workflow for all of the candidates. For this reason, we used our deep learning property prediction tool (ALIGNN) to screen all 3000 candidate materials. ALIGNN has demonstrated success for predicting properties such as formation energy and band gap and more recently superconducting  $T_c$ . The screening criteria we established for further investigation of these candidates was an ALIGNN predicted:  $T_c > 5$  K,  $E_{\text{form}} < 0$  eV/atom, and  $E_{\text{gap}} < 0.05$  eV. This criterion is based on the fact that we want to further investigate superconducting materials which have a high  $T_c$ , are potentially stable, and are metallic (high density of states at the Fermi level). Although negative formation energy is a stringent requirement for stability, investigations of dynamical and thermodynamic stability are still needed to confirm stability (phonon spectrum and energy above the convex hull). After performing this screening with ALIGNN, we found 62 materials which fit this criterion. We then went on to perform the full DFT-EPC workflow for these 62 materials and computed the  $T_c$  using the McMillan-Allen-Dynes equation. After computing the  $T_c$  of these materials with DFT, we found that 32 structures have a  $T_c$  above 5 K. Upon investigation of the phonon density of states and chemical composition, we find that 12 of these structures have either negative phonon frequencies, indicating dynamical instability, or have a chemical composition already in the JARVIS training set. The remaining 20 candidate superconductors are presented in Table 1.

Before discussing the more detailed results of the 20 new candidate superconducting materials generated by our workflow depicted in Fig. 1a), we will discuss the intermediate steps of the workflow in more detail. The CDVAE model has the capability to produce new structures with chemical and structural diversity. Fig. 1b) depicts the probability that compounds containing a given element in the 3000 CDVAE generated structures have an

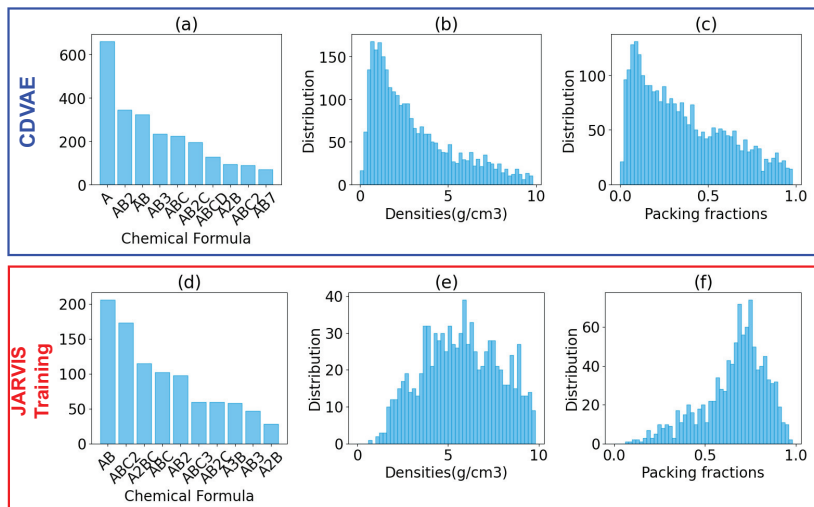


Figure 2: The chemical formula, distribution of densities, and distribution of packing fractions for a) - c) the 3000 CDVAE generated structures and for d) - f) the 1058 structures used for training from the JARVIS-DFT database.

ALIGNN predicted  $T_C$  above 3 K (displayed as a heat map overlaid on the periodic table). We observe that compounds containing C, N, B, O, V, Mn, Nb, Ru, and Ta are the most abundant with regards to structures that have a higher predicted  $T_c$  with ALIGNN. This is not surprising, due to the fact that several of the materials in the DFT training set that have a high value of  $T_c$  contain such elements (see ref. <sup>6</sup> for details).

Although the abundance of elements in the CDVAE structures (with an ALIGNN predicted  $T_c > 3$  K) follows similar trends to the training data, the CDVAE candidate structures are not restricted to stoichiometries and crystal structures already present in the training data. This is illustrated by Fig. 2, where the chemical formula, distribution of densities, and distribution of packing fractions for a) - c) the 3000 CDVAE generated structures and for d) - f) the 1058 structures used for training from the JARVIS-DFT database is depicted. A comparison of Fig. 2a) and 2d) emphasizes the difference in the stoichiometry between the CDVAE generated structures and the training data from JARVIS. For example, in the JARVIS training set, a majority of the data contains only three different atomic species (A, B, and C) and the unit cells have 5 formula units (see Fig. 2d)). In contrast, the CDVAE generated data based on the JARVIS training set see Fig. 2a)) has a number of structures



that contain four atomic species (A, B, C, D) and unit cells that have a larger number of formula units (i.e.,  $AB_7$ ). In addition, the CDVAE generated data contains a substantial number of monoelemental structures, while this is not a prevalent component in the training set. When comparing Fig. 2b) and 2e) and 2c) and 2f), we observe very different distributions for densities and packing fractions between the CDVAE structures and JARVIS training data. Specifically, the CDVAE generated structures have a much larger distribution of structures with a low density and packing fraction. This can be due in part to the low symmetry of the CDVAE generated structures, which gives rise to larger crystal volumes for the newly generated unit cells and therefore smaller densities and packing fractions. In fact, the CDVAE structures are all of space group P1. The likelihood of the CDVAE model generating low symmetry, chemically diverse structures might be attributed to the CDVAE model sampling from a Gaussian distribution to create new materials (to predict the number of atoms and composition). Since the underlying distribution of the materials is non-Gaussian, and the Gaussian distribution that the CDVAE model samples from is not representative of the latent space, materials out of the distribution can be generated. This is a limitation of CDVAE which could be addressed with a better latent space encoding in the future.

After discussing the structural and chemical diversity of the CDVAE generated structures, we plan to discuss the steps of the workflow that involve the prediction of  $T_c$  with deep learning (ALIGNN) and DFT. The ALIGNN deep learning property predictor for  $T_c$  was previously pretrained on the JARVIS dataset in ref.<sup>6</sup> and benchmarked. Using the pretrained ALIGNN model allows us to filter the vast amount of CDVAE candidate superconductors with instantaneous property prediction. Fig. 3a) and b) depict the distribution of  $T_C$  for the a) 1058 JARVIS-DFT structures ( $T_C$  computed with DFT) and b) the 3000 CDVAE structures ( $T_C$  computed with ALIGNN). As seen in the figure, the distribution of  $T_c$  is vastly different. Most strikingly, the CDVAE generated data has a very low amount of structures with a predicted  $T_c$  close to zero (non-superconducting), as opposed to a large number of materials in the JARVIS training set that have a  $T_c$  close to zero. In addition, the

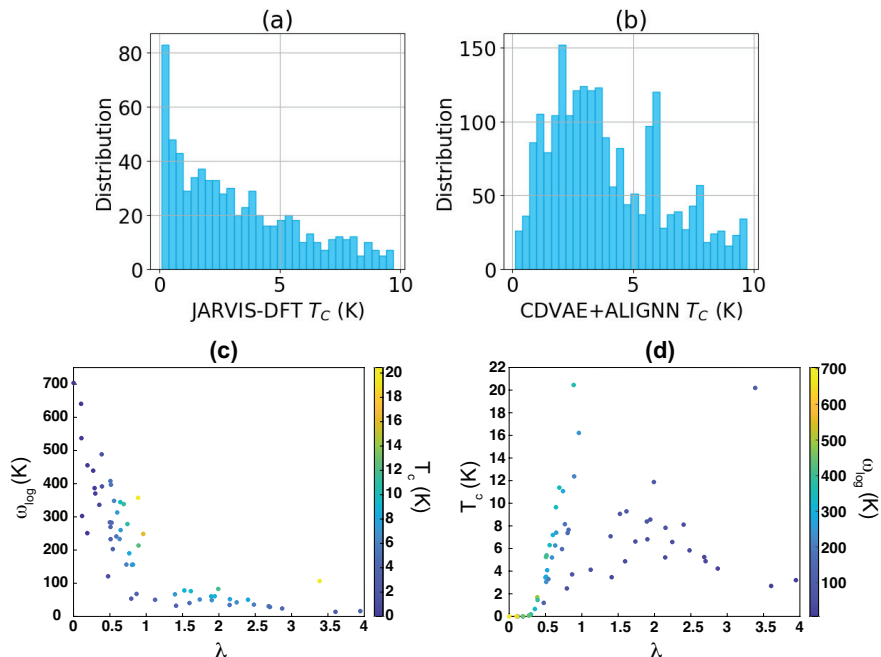


Figure 3: The distribution of  $T_C$  for the a) 1058 JARVIS-DFT structures ( $T_C$  computed with DFT) and b) the 3000 CDVAE structures ( $T_C$  computed with ALIGNN). c) - d) the relation between EPC parameters for the CDVAE candidate materials verified with DFT.

distribution of CDVAE+ALIGNN temperatures resembles more of a Gaussian distribution, with a majority of the  $T_c$  values of the newly generated structures concentrated around 2.5 K - 6 K. This can be an indicator of the success of the CDVAE model for generating new structures with an optimized target property, such as  $T_c$ , in the latent space.

After screening the 3000 CDVAE generated structures with ALIGNN, we performed DFT for the 62 candidates that met the ALIGNN screening criteria depicted in Fig. 1a). At this stage, it is important to acknowledge the success of the pretrained ALIGNN model with regards to predicting the  $T_c$  of these newly generated structures. Out of the 62 structures, 58 of them have a DFT computed  $T_c > 0$  K, which indicates that ALIGNN is 87 % successful with filtering out superconducting materials from the CDVAE generated structures. Out of the 62 structures, 32 of them have a DFT computed  $T_c > 5$  K, which indicates that ALIGNN has a 52 % success rate in filtering out materials with a  $T_c$  above 5 K from the CDVAE generated structures. The success of the ALIGNN prediction of  $T_c$  is a direct consequence of the availability of training data. In terms of deep learning models for material property

prediction, 1058 structures is a relatively small amount of data to train on. The reason for the smaller training set size is due to the vast computational expense needed to perform these DFT calculations of EPC properties. In principle, the ALIGNN prediction of  $T_c$  can be systematically improved by adding more DFT calculations to the training, which is an ongoing effort of JARVIS. We show the relationship between EPC parameters ( $\lambda$ ,  $\omega_{\log}$ ,  $T_c$ ) for the 62 materials we performed DFT calculations for in Fig. 3c) and d). Fig. 3c) depicts an inverse relationship between  $\lambda$  and  $\omega_{\log}$  and in Fig. 3d), we observe a somewhat positive relationship between  $\lambda$  and  $T_c$ . These are typical behaviors of BCS superconductors and were observed in our work on BCS bulk and 2D superconductors.<sup>6,7</sup> From the colormap of Fig. 3c) and d), it is clear that a balance of high  $\lambda$  and  $\omega_{\log}$  is a necessary condition for a material to have a high  $T_c$ .

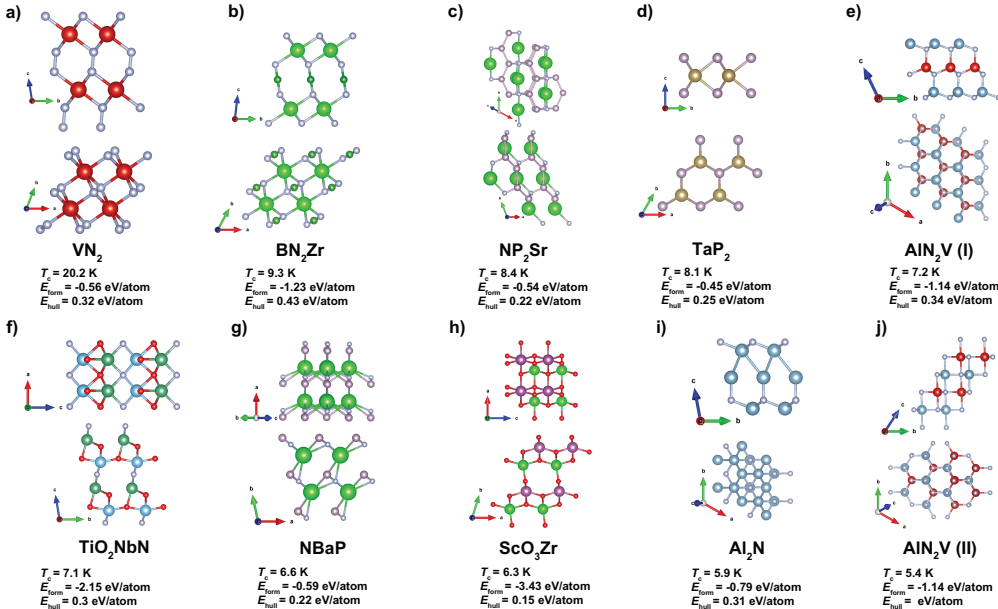


Figure 4: Top and side view of the top superconductor candidates (closest to the convex hull) generated with CDVAE and verified with DFT: a)  $\text{VN}_2$ , b)  $\text{BN}_2\text{Zr}$ , c)  $\text{NP}_2\text{Sr}$ , d)  $\text{TaP}_2$ , e)  $\text{AlN}_2\text{V (I)}$ , f)  $\text{TiO}_2\text{NbN}$ , g)  $\text{NBaP}$ , h)  $\text{ScO}_3\text{Zr}$ , i)  $\text{Al}_2\text{N}$  and j)  $\text{AlN}_2\text{V (II)}$ .  $T_c$ ,  $E_{\text{form}}$  and  $E_{\text{hull}}$  are also given for each material.

Out of the 62 newly generated materials we ran DFT for, 32 had a computed  $T_c$  above 5 K. We went on to further examine the phonon properties and chemical composition of these materials and found that 12 of these structures possessed either negative phonon modes

Table 1: Chemical formula, JARVIS ID (JID),  $T_C$ , formation energy per atom and energy above the convex hull per atom of the 20 candidate superconductors from CDVAE verified by DFT calculations.

Structure	JID	$T_C$ (K)	$E_{\text{form}}$ (eV/atom)	$E_{\text{hull}}$ (eV/atom)
VN <sub>2</sub>	JVASP-161655	20.2	-0.56	0.32
NTaB (I)	JVASP-161630	16.2	-0.32	0.84
BORu	JVASP-161610	12.4	-0.72	0.75
BTa <sub>2</sub> N	JVASP-161612	11.9	-0.37	0.67
NTaB (II)	JVASP-161624	11.1	-0.32	0.84
BN <sub>2</sub> Zr	JVASP-161608	9.3	-1.23	0.43
BTaNS	JVASP-161613	9.1	-0.33	0.88
NP <sub>2</sub> Sr	JVASP-162663	8.4	-0.54	0.22
TaP <sub>2</sub>	JVASP-161649	8.1	-0.45	0.25
NPdTi <sub>2</sub>	JVASP-161629	7.7	-0.78	0.47
PScSi <sub>2</sub>	JVASP-161644	7.4	-0.43	0.49
AlN <sub>2</sub> V (I)	JVASP-161599	7.2	-1.14	0.34
TiO <sub>2</sub> NbN	JVASP-161653	7.1	-2.15	0.30
NBaP	JVASP-161626	6.6	-0.59	0.22
NVBRu	JVASP-161631	6.3	-0.14	0.74
ScO <sub>3</sub> Zr	JVASP-161647	6.3	-3.43	0.15
Al <sub>2</sub> N	JVASP-161597	5.9	-0.79	0.31
AlN <sub>2</sub> V (II)	JVASP-162662	5.4	-1.14	0.34
ScBORuCa	JVASP-161646	5.2	-1.12	0.58
B <sub>2</sub> TaS	JVASP-161604	5.2	-0.07	0.58

(indicating dynamical instability) or had a chemical composition already in the JARVIS training set. The top 20 new superconducting candidates are displayed in Table 1. The chemical composition,  $T_c$ , formation energy per atom and energy above the convex hull are given in Table 1. As seen in the table, all of the 20 structures have negative formation energy. Although negative formation energy is a necessary prerequisite for thermodynamic stability, it does not guarantee thermodynamic stability. For this reason, we calculated the energy above the convex hull (shown in Table 1). We computed the convex hull of these structures from the formation energy calculations of the different phases in JARVIS-DFT. From here,

we observed 10 structures within an energy of 0.45 eV or less from the convex hull, and deem that these structures are the most likely to be experimentally synthesized. The atomic structures (all of P1 symmetry) of these 10 materials are given in Fig. 4 ( $\text{VN}_2$ ,  $\text{BN}_2\text{Zr}$ ,  $\text{NP}_2\text{Sr}$ ,  $\text{TaP}_2$ ,  $\text{AlN}_2\text{V}$  (I),  $\text{TiO}_2\text{NbN}$ ,  $\text{NBaP}$ ,  $\text{ScO}_3\text{Zr}$ ,  $\text{Al}_2\text{N}$ ,  $\text{AlN}_2\text{V}$  (II)). The properties and atomic structures of all the materials we performed DFT verification for (62 materials) will be available along with this manuscript and uploaded to the JARVIS-DFT database (<https://jarvis.nist.gov/>). Although these 10 materials have an energy above the convex hull between 0.22 eV/atom and 0.43 eV/atom, indicating that thermodynamic stability is still not guaranteed, they still may be synthesizable. In fact, Aykol et al.<sup>54</sup> demonstrated that nitride-based polymorphs with a higher energy above the convex hull can be stable up to a high energetic amorphous limit. Since a majority of these superconductors contain nitrogen, this gives promise that they can eventually be experimentally realized.

As a success metric of the CDVAE method for inverse design, it is important to measure how diverse the chemical composition and crystal structure of the generated materials are, not only with respect to the training data, but with respect to larger areas of phase space. As previously mentioned, these top 20 candidate superconductors do not have a chemical composition in the training set. In addition, we searched the entire JARVIS database (over 70000 structures) for materials with the same stoichiometry as the top 20 candidates and found no such structures. Due to the fact that the JARVIS database has less materials (the primary focus of JARVIS is to expand the properties and accuracy of materials), we checked other well-established materials databases for these candidates. Specifically, we checked the Materials Project (over 150000 structures) and OQMD (over 1000000 structures). For  $\text{VN}_2$ , we found 3 compounds in OQMD with entirely different structures (1239835, 1233906, 1589664) with  $E_{\text{hull}}$  ranging from 0.8 to 2.6 eV/atom. For  $\text{Al}_2\text{N}$ , we found 4 compounds in OQMD with entirely different structures (1237731, 1415673, 1590028) with  $E_{\text{hull}}$  ranging from (0.9 to 2.6) eV/atom. We found 3  $\text{TaP}_2$  compounds (1372133, 1590238, 1237725) in OQMD. The  $E_{\text{hull}}$  ranged from 0 to 1.2 eV/atom, but none of these phases

resemble the structure in this study, which has a similar crystal structure to layered transition metal dichalcogenides (such as 2H-MoS<sub>2</sub>). We found 1 AlN<sub>2</sub>V compound in the Materials Project (mp-1247742), where the  $E_{\text{hull}}$  was 0.37 eV/atom. When comparing this structure to the two AlN<sub>2</sub>V structures in our study, mp-1247742 has a similar form to AlN<sub>2</sub>V (I) but a drastically different structure than AlN<sub>2</sub>V (II). We additionally searched the Supercon database (the Supercon database is unavailable as of December 2021, but previous papers have made this dataset available for further research<sup>55,56</sup>), which consists of over 16000 experimentally realized superconducting materials. We find no common materials between the top 20 CDVAE candidates and the Supercon database. This further proves that the CDVAE method can generate unique materials with a specific desired property, covering previously undiscovered areas of phase space.

In this work, we used a multi step workflow, combining generative models, deep learning property prediction and DFT to discover next-generation superconducting materials. We demonstrated that the deep learning property prediction using the ALIGNN model can accelerate the search for new superconductors by instantaneously screening the properties of the newly generated materials prior to DFT verification and experimental investigation. Our search revealed 20 newly predicted candidate superconductors, with 10 structures being close to the convex hull and  $T_c$  values as high as 20.2 K. Our approach goes beyond the standard funnel-like materials design workflow and allows for inverse design of novel materials, populating previously undiscovered areas of phase space.

## Data Availability Statement

The data from the present work is available as a part of the JARVIS-DFT database (<https://jarvis.nist.gov/>).

## Code Availability Statement

Software packages mentioned in the article can be found at <https://github.com/usnistgov/jarvis> and <https://github.com/txie-93/cdvae>.

## Competing interests

The authors declare no competing interests.

## Acknowledgments

All authors thank the National Institute of Standards and Technology for funding, computational, and data-management resources, specifically the NIST Nisaba and Raritan HPC clusters. K.C. thanks the computational support from XSEDE (Extreme Science and Engineering Discovery Environment) computational resources under allocation number TG-DMR 190095. Contributions from K.C. were supported by the financial assistance award 70NANB19H117 from the U.S. Department of Commerce, National Institute of Standards and Technology.

## References

- (1) Kamerlingh Onnes, H. The resistance of pure mercury at helium temperatures. *Commun. Phys. Lab. Univ. Leiden*, b **1911**, 120.
- (2) Poole, C. P.; Farach, H. A.; Creswick, R. J. *Superconductivity*; Academic press, 2013.
- (3) Rogalla, H.; Kes, P. H. *100 years of superconductivity*; Taylor & Francis, 2011.
- (4) Cooper, L. N.; Feldman, D. *BCS: 50 years*; World scientific, 2010.

- (5) Giustino, F. Electron-phonon interactions from first principles. *Reviews of Modern Physics* **2017**, *89*, 015003.
- (6) Choudhary, K.; Garrity, K. Designing high-TC superconductors with BCS-inspired screening, density functional theory, and deep-learning. *npj Computational Materials* **2022**, *8*, 244.
- (7) Wines, D.; Choudhary, K.; Biacchi, A. J.; Garrity, K. F.; Tavazza, F. High-Throughput DFT-Based Discovery of Next Generation Two-Dimensional (2D) Superconductors. *Nano Letters* **2023**, *23*, 969–978.
- (8) Jain, A.; Ong, S. P.; Hautier, G.; Chen, W.; Richards, W. D.; Dacek, S.; Cholia, S.; Gunter, D.; Skinner, D.; Ceder, G.; Persson, K. A. Commentary: The Materials Project: A materials genome approach to accelerating materials innovation. *APL Materials* **2013**, *1*, 011002.
- (9) Saal, J. E.; Kirklin, S.; Aykol, M.; Meredig, B.; Wolverton, C. Materials Design and Discovery with High-Throughput Density Functional Theory: The Open Quantum Materials Database (OQMD). *JOM* **2013**, *65*, 1501–1509.
- (10) Kirklin, S.; Saal, J. E.; Meredig, B.; Thompson, A.; Doak, J. W.; Aykol, M.; Rühl, S.; Wolverton, C. The Open Quantum Materials Database (OQMD): assessing the accuracy of DFT formation energies. *npj Computational Materials* **2015**, *1*, 15010.
- (11) Hastrup, S.; Strange, M.; Pandey, M.; Deilmann, T.; Schmidt, P. S.; Hinsche, N. F.; Gjerding, M. N.; Torelli, D.; Larsen, P. M.; Riis-Jensen, A. C.; Gath, J.; Jacobsen, K. W.; Mortensen, J. J.; Olsen, T.; Thygesen, K. S. The Computational 2D Materials Database: high-throughput modeling and discovery of atomically thin crystals. *2D Materials* **2018**, *5*, 042002.
- (12) Gjerding, M. N. et al. Recent progress of the Computational 2D Materials Database (C2DB). *2D Materials* **2021**, *8*, 044002.



- (13) Choudhary, K.; Garrity, K. F.; Reid, A. C.; DeCost, B.; Biacchi, A. J.; Hight Walker, A. R.; Trautt, Z.; Hatrick-Simpers, J.; Kusne, A. G.; Centrone, A., et al. The joint automated repository for various integrated simulations (JARVIS) for data-driven materials design. *npj Computational Materials* **2020**, *6*, 1–13.
- (14) Ong, S. P.; Richards, W. D.; Jain, A.; Hautier, G.; Kocher, M.; Cholia, S.; Gunter, D.; Chevrier, V. L.; Persson, K. A.; Ceder, G. Python Materials Genomics (pymatgen): A robust, open-source python library for materials analysis. *Computational Materials Science* **2013**, *68*, 314–319.
- (15) Ramesh, A.; Pavlov, M.; Goh, G.; Gray, S.; Voss, C.; Radford, A.; Chen, M.; Sutskever, I. Zero-Shot Text-to-Image Generation. 2021.
- (16) Wu, K. E.; Yang, K. K.; van den Berg, R.; Zou, J. Y.; Lu, A. X.; Amini, A. P. Protein structure generation via folding diffusion. 2022.
- (17) Xie, T.; Fu, X.; Ganea, O.-E.; Barzilay, R.; Jaakkola, T. Crystal Diffusion Variational Autoencoder for Periodic Material Generation. 2021; <https://arxiv.org/abs/2110.06197>.
- (18) Lyngby, P.; Thygesen, K. S. Data-driven discovery of 2D materials by deep generative models. *npj Computational Materials* **2022**, *8*, 232.
- (19) Moustafa, H.; Lyngby, P. M.; Mortensen, J. J.; Thygesen, K. S.; Jacobsen, K. W. Hundreds of new, stable, one-dimensional materials from a generative machine learning model. *Phys. Rev. Mater.* **2023**, *7*, 014007.
- (20) Fung, V.; Jia, S.; Zhang, J.; Bi, S.; Yin, J.; Ganesh, P. Atomic structure generation from reconstructing structural fingerprints. *Machine Learning: Science and Technology* **2022**, *3*, 045018.

- (21) Noh, J.; Gu, G. H.; Kim, S.; Jung, Y. Machine-enabled inverse design of inorganic solid materials: promises and challenges. *Chem. Sci.* **2020**, *11*, 4871–4881.
- (22) Kim, S.; Noh, J.; Gu, G. H.; Aspuru-Guzik, A.; Jung, Y. Generative Adversarial Networks for Crystal Structure Prediction. *ACS Central Science* **2020**, *6*, 1412–1420.
- (23) Long, T.; Fortunato, N. M.; Opahle, I.; Zhang, Y.; Samathrakris, I.; Shen, C.; Gutfleisch, O.; Zhang, H. Constrained crystals deep convolutional generative adversarial network for the inverse design of crystal structures. *npj Computational Materials* **2021**, *7*, 66.
- (24) Song, Y.; Siriwardane, E. M. D.; Zhao, Y.; Hu, J. Computational Discovery of New 2D Materials Using Deep Learning Generative Models. *ACS Applied Materials & Interfaces* **2021**, *13*, 53303–53313.
- (25) Noh, J.; Kim, J.; Stein, H. S.; Sanchez-Lengeling, B.; Gregoire, J. M.; Aspuru-Guzik, A.; Jung, Y. Inverse Design of Solid-State Materials via a Continuous Representation. *Matter* **2019**, *1*, 1370–1384.
- (26) Zhao, Y.; Al-Fahdi, M.; Hu, M.; Siriwardane, E. M. D.; Song, Y.; Nasiri, A.; Hu, J. High-Throughput Discovery of Novel Cubic Crystal Materials Using Deep Generative Neural Networks. *Advanced Science* **2021**, *8*, 2100566.
- (27) Ren, Z. et al. An invertible crystallographic representation for general inverse design of inorganic crystals with targeted properties. *Matter* **2022**, *5*, 314–335.
- (28) Kingma, D. P.; Welling, M. Auto-Encoding Variational Bayes. 2013; <https://arxiv.org/abs/1312.6114>.
- (29) Sohl-Dickstein, J.; Weiss, E.; Maheswaranathan, N.; Ganguli, S. Deep Unsupervised Learning using Nonequilibrium Thermodynamics. Proceedings of the 32nd International Conference on Machine Learning. Lille, France, 2015; pp 2256–2265.

- (30) Song, Y.; Ermon, S. Generative Modeling by Estimating Gradients of the Data Distribution. 2019; <https://arxiv.org/abs/1907.05600>.
- (31) Sohl-Dickstein, J.; Weiss, E. A.; Maheswaranathan, N.; Ganguli, S. Deep Unsupervised Learning using Nonequilibrium Thermodynamics. 2015.
- (32) Batzner, S.; Musaelian, A.; Sun, L.; Geiger, M.; Mailoa, J. P.; Kornbluth, M.; Molinari, N.; Smidt, T. E.; Kozinsky, B. E(3)-equivariant graph neural networks for data-efficient and accurate interatomic potentials. *Nature Communications* **2022**, *13*, 2453.
- (33) Choudhary, K.; DeCost, B. Atomistic Line Graph Neural Network for improved materials property predictions. *npj Computational Materials* **2021**, *7*, 1–8.
- (34) Paszke, A.; Gross, S.; Massa, F.; Lerer, A.; Bradbury, J.; Chanan, G.; Killeen, T.; Lin, Z.; Gimelshein, N.; Antiga, L., et al. Pytorch: An imperative style, high-performance deep learning library. *Advances in neural information processing systems* **2019**, *32*, 8026–8037.
- (35) Wang, M.; Yu, L.; Zheng, D.; Gan, Q.; Gai, Y.; Ye, Z.; Li, M.; Zhou, J.; Huang, Q.; Ma, C., et al. Deep Graph Library: Towards Efficient and Scalable Deep Learning on Graphs. *arXiv e-prints* **2019**,
- (36) Choudhary, K.; Zhang, Q.; Reid, A. C.; Chowdhury, S.; Van Nguyen, N.; Trautt, Z.; Newrock, M. W.; Congo, F. Y.; Tavazza, F. Computational screening of high-performance optoelectronic materials using OptB88vdW and TB-mBJ formalisms. *Scientific data* **2018**, *5*, 1–12.
- (37) Choudhary, K.; Bercx, M.; Jiang, J.; Pachter, R.; Lamoen, D.; Tavazza, F. Accelerated discovery of efficient solar cell materials using quantum and machine-learning methods. *Chemistry of Materials* **2019**, *31*, 5900–5908.

- (38) Choudhary, K.; Garrity, K. F.; Ghimire, N. J.; Anand, N.; Tavazza, F. High-throughput search for magnetic topological materials using spin-orbit spillage, machine learning, and experiments. *Physical Review B* **2021**, *103*, 155131.
- (39) Choudhary, K.; Garrity, K. F.; Tavazza, F. High-throughput discovery of topologically non-trivial materials using spin-orbit spillage. *Scientific reports* **2019**, *9*, 1–8.
- (40) Choudhary, K.; Garrity, K. F.; Jiang, J.; Pachter, R.; Tavazza, F. Computational search for magnetic and non-magnetic 2D topological materials using unified spin-orbit spillage screening. *NPJ Computational Materials* **2020**, *6*, 1–8.
- (41) Choudhary, K.; Cheon, G.; Reed, E.; Tavazza, F. Elastic properties of bulk and low-dimensional materials using van der Waals density functional. *Physical Review B* **2018**, *98*, 014107.
- (42) Choudhary, K.; Garrity, K. F.; Sharma, V.; Biacchi, A. J.; Hight Walker, A. R.; Tavazza, F. High-throughput density functional perturbation theory and machine learning predictions of infrared, piezoelectric, and dielectric responses. *NPJ Computational Materials* **2020**, *6*, 1–13.
- (43) Choudhary, K.; Ansari, J. N.; Mazin, I. I.; Sauer, K. L. Density functional theory-based electric field gradient database. *Scientific Data* **2020**, *7*, 1–10.
- (44) Choudhary, K.; Kalish, I.; Beams, R.; Tavazza, F. High-throughput identification and characterization of two-dimensional materials using density functional theory. *Scientific reports* **2017**, *7*, 1–16.
- (45) Wines, D.; Choudhary, K.; Tavazza, F. Systematic DFT+U and Quantum Monte Carlo Benchmark of Magnetic Two-Dimensional (2D) CrX<sub>3</sub> (X = I, Br, Cl, F). *The Journal of Physical Chemistry C* **2023**, *127*, 1176–1188.

- (46) Choudhary, K.; Tavazza, F. Convergence and machine learning predictions of Monkhorst-Pack k-points and plane-wave cut-off in high-throughput DFT calculations. *Computational materials science* **2019**, *161*, 300–308.
- (47) Baroni, S.; Giannozzi, P.; Testa, A. Green’s-function approach to linear response in solids. *Physical review letters* **1987**, *58*, 1861.
- (48) Gonze, X. Perturbation expansion of variational principles at arbitrary order. *Physical Review A* **1995**, *52*, 1086.
- (49) Wierzbowska, M.; de Gironcoli, S.; Giannozzi, P. Origins of low-and high-pressure discontinuities of  $T_{c}$  in niobium. *arXiv preprint cond-mat/0504077* **2005**,
- (50) Giannozzi, P.; Baroni, S.; Bonini, N.; Calandra, M.; Car, R.; Cavazzoni, C.; Ceresoli, D.; Chiarotti, G. L.; Cococcioni, M.; Dabo, I., et al. QUANTUM ESPRESSO: a modular and open-source software project for quantum simulations of materials. *Journal of physics: Condensed matter* **2009**, *21*, 395502.
- (51) Perdew, J. P.; Ruzsinszky, A.; Csonka, G. I.; Vydrov, O. A.; Scuseria, G. E.; Constantin, L. A.; Zhou, X.; Burke, K. Restoring the density-gradient expansion for exchange in solids and surfaces. *Physical review letters* **2008**, *100*, 136406.
- (52) Garrity, K. F.; Bennett, J. W.; Rabe, K. M.; Vanderbilt, D. Pseudopotentials for high-throughput DFT calculations. *Computational Materials Science* **2014**, *81*, 446–452.
- (53) McMillan, W. Transition temperature of strong-coupled superconductors. *Physical Review* **1968**, *167*, 331.
- (54) Aykol, M.; Dwaraknath, S. S.; Sun, W.; Persson, K. A. Thermodynamic limit for synthesis of metastable inorganic materials. *Science Advances* **2018**, *4*, eaaq0148.
- (55) vstanev1, Supercon. 2021; <https://github.com/vstanev1/Supercon>.

- (56) Hamidieh, K. A Data-Driven Statistical Model for Predicting the Critical Temperature of a Superconductor. 2018.

TOC graphic

